Journal of The Electrochemical Society, **157** (3) E31-E35 (2010)
0013-4651/2010/157(3)/E31/5/$28.00 © The Electrochemical Society

A Solid-State Electrochemical Reaction as the Origin of Magnetism at Oxide Nanoparticle Interfaces

Marisol S. Martin-González,[a,z] Miguel A. García,[b,c] Israel Lorite,[c] José L. Costa-Krämer,[a] Fernando Rubio-Marcos,[c] N. Carmona,[b] and José F. Fernández[c]

[a]*Instituto de Microelectrónica de Madrid, Centro Nacional de Microelectrónica, Consejo Superior de Investigaciones Científicas, 28760 Madrid, Spain*
[b]*Departamento de Física de Materiales, Universidad Complutense de Madrid, 28940 Madrid, Spain*
[c]*Instituto de Cerámica y Vidrio, Consejo Superior de Investigaciones Científicas, 28049 Madrid, Spain*

Solid oxide interfaces are at the forefront of solid-state science and materials research, exhibiting very appealing properties for new devices. This work describes the appearance of unexpected magnetic phenomena related to solid-state redox reaction, which might be the origin of the recently discovered magnetic signals in oxide multilayers and ceramic mixtures. The magnetic signal arises only when dissimilar oxide nanoparticles are simply mixed at room temperature, and it is not observed when nanoparticles are of the same chemical composition. Therefore, the phenomenon is ascribed to an interfacial solid-state reaction. Raman and X-ray absorption spectroscopies, scanning electron microscopy, and vibrating sample magnetometer have allowed us to identify the origin of the ferrimagnetic response. It is due to an electrochemical surface reduction of Co^{3+} in octahedral coordination to Co^{2+}. So, $Co^{2+}_{(oct)}$–O–$Co^{2+}_{(tetra)}$ interactions are produced. The reaction is driven by the different surface basicity of the oxides and has allowed obtaining different degrees of reaction, and concomitantly a proportionally strong magnetic response, when Co_3O_4 nanoparticles are mixed with SiO_2, Al_2O_3, TiO_2, and ZnO (from a larger to a smaller ferrimagnetic response). Also, a mechanism by which Co_3O_4 nanoparticles become ferrimagnetic is proposed.
 [DOI: 10.1149/1.3272638]

Manuscript submitted July 8, 2009; revised manuscript received September 24, 2009. Published January 12, 2010.

Interesting properties are starting to be found at the interface of two dissimilar transition-metal oxides due to proximity and indiffusion phenomena.[1-3] For instance, high conducting (electron gas),[4] superconductivity,[5] or magnetic interfaces have been recently discovered in carefully controlled, atomically smooth interfaces of oxides[6] prepared by high vacuum deposition techniques. Among them, magnetic ordering is a hot topic in solid-state science. Its underlying mechanisms are still the subject of intense research. Because the magnetic measurements provide an overall magnetic moment that includes bulk and nanoscale contributions, it is quite difficult to assign it to a particular material structure. In particular, the interplay between localized magnetic moments and the spin of itinerant conduction electrons in a solid gives rise to intriguing many-body effects such as Ruderman–Kittel–Kasuya–Yosida interactions,[7] the Kondo effect,[8] or carrier-induced ferromagnetism in diluted magnetic semiconductors (DMSs),[9] with potential application in the field of spintronics. The oxide interface now provides a versatile system to induce and manipulate magnetic moments in otherwise nonmagnetic materials, which is nowadays one of the most active and pursued goals of material physics and chemistry.[10]

The appearance of magnetism in a priori nonmagnetic oxides has been observed in the so-called DMSs. Recent results[11-14] indicate that the appearance of magnetism in these oxides (mainly ZnO and TiO_2) is related to the presence of defects and surface/interface effects.[1,4,15-18] The experimental observations show very weak magnetic signals, suggesting that only few atoms are responsible for the measured ferromagnetism. The results are hardly reproducible, and findings from different groups are commonly contradictory. Moreover, the mechanisms that explain its origin and how it can be produced and enhanced have not been described yet.

In this work, it is shown that these properties can be obtained as a consequence of the high surface reactivity of the oxide nanoparticles. A simple process consisting of low energy mixing of two nonmagnetic oxides for few minutes at room temperature can induce the formation of interfaces with magnetic properties. The reaction mechanism and a model of how a nonmagnetic oxide can become magnetic are presented.

[z] E-mail: marisol@imm.cnm.csic.es

Experimental

The low energy oxide mixing consisted of a process where 5 g of a mixture of 99 wt % ZnO, TiO_2, Al_2O_3, or SiO_2 particles and 1 wt % of Co_3O_4 nanoparticles were shaken in a 60 cm^3 nylon container for 5 min at 500 rpm using a turbula-type mixer. The process was done with 1 mm balls. The pure powders were also measured to ensure that no ferromagnetic contributions were due to the mixing process. Analytical grade powders were dried at 110°C for 2 h before dry mixing. All processes were performed avoiding any contact with metal surfaces such as spatulas or tweezers to avoid any metallic contamination.[19] All the Co_3O_4 used in this work was precalcinated at 400°C to avoid possible contributions of metallic cobalt.[15,17]

Magnetic properties were measured in a high temperature vibrating sample magnetometer (VSM) above room temperature. To increase the magnetic signal and to keep the experimental uncertainty down to 5%, samples of 3 g weight of each composition were measured. They consisted of ball pellets of isostatically pressed powders. Separated reference powders were measured the same way to rule out magnetic impurity effects.

Raman spectra were collected on a Renishaw Micro-Raman System 1000. The samples were excited with the 514 nm argon line.

Results and Discussion

A mixture of ZnO with Co_3O_4 nanoparticles is shown in Fig. 1a. The micrograph reveals Co_3O_4 nanoparticles adhered to the ZnO surfaces. A large number of interfaces between dissimilar oxides are observed and a few of them appear agglomerated. A simple dry mixing process produces such a dispersion of the previously highly agglomerated Co_3O_4 nanoparticles. In this sense, it seems that the larger ZnO particles act as grinding media for the smaller Co_3O_4 nanoparticles. The dispersion and adherence of nanoparticles would indicate that a spontaneous reaction occurs at room temperature between these materials. Many works pursue an effective nanoparticle dispersion and use liquid media, which form a double electrostatic layer that inhibits the spontaneous reactions reported here. This effect has also been observed for other mixtures of Co_3O_4 with other semiconductors such as $TiO_{2(anatase)}$,[18] and in mixtures with other insulating materials such as Al_2O_3 particles or SiO_2 film, and it is shown in Fig. 1c and d, respectively.

In a previous work, it was shown that no variations in the X-ray

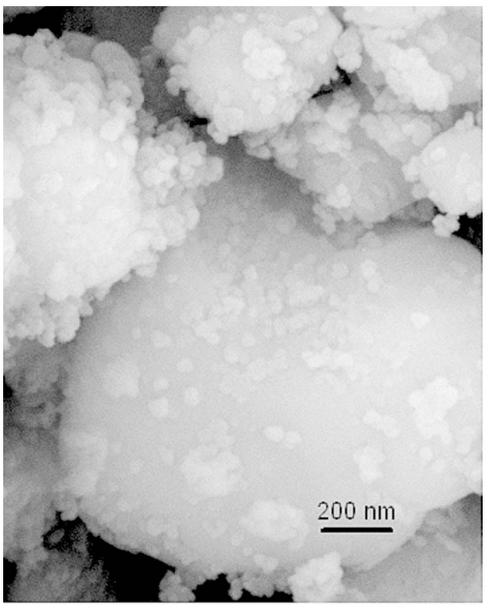

(a)

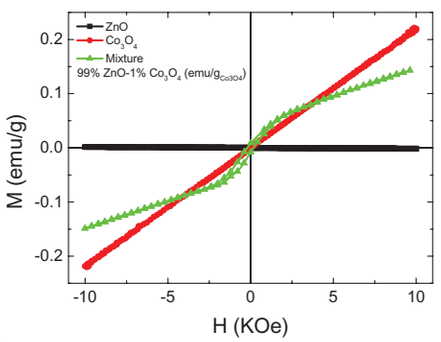

(b)

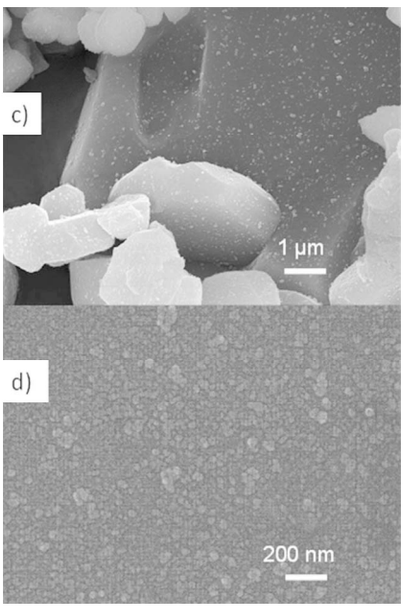

Figure 1. (Color online) (a) Field-emission-scanning electron microscopy micrograph of ZnO particles covered by Co_3O_4 nanoparticles adhered at the surface after low energy mixing. (b) Magnetization curves at 300 K from pure ZnO, Co_3O_4 nanoparticles, and a mixture of 99% ZnO–1% Co_3O_4 (mol). The curve for the last sample is presented in emu/g Co_3O_4 for clarity. (c) Co_3O_4 nanoparticles dispersed over Al_2O_3 particles. (d) Co_3O_4 nanoparticles randomly distributed on a SiO_2 film on a Si single crystal.

diffractograms or in the high resolution transmission electron micrograph are observed after mixing without further thermal treatment.[15,17,18] But, when the magnetization curves are measured, a clear ferromagnetic-like behavior at room temperature appears in these mixtures of diamagnetic and paramagnetic oxides,[17,15] see Fig. 1b. In this sense, optical measurements are also useful for the investigation of surface effects because they are particularly sensitive to the material surface.

The changes in the Co_3O_4 nanoparticles can be followed by Raman spectroscopy. A displacement of the bands is observed after mixing Co_3O_4 with ZnO when compared with pure Co_3O_4, see Fig. 2. This displacement has been previously interpreted as a surface reduction of the Co_3O_4 nanoparticles to CoO.[15] This displacement is more noticeable for mixtures Al_2O_3/Co_3O_4 and even more for SiO_2/Co_3O_4. This is consistent with a surface reduction that is more intense for the case of SiO_2 than that for Al_2O_3 and ZnO.

For further confirmation of the Co_3O_4 surface reduction as the origin of the ferromagnetic signal, X-ray absorption spectroscopy measurements at the Co K-edge were performed for Co_3O_4, ZnO–Co_3O_4 (1%), and $TiO_{2(anatase)}$–Co_3O_4 (1%). The shape of the edge is similar for the three cases, see Fig. 3. However, for ZnO–Co_3O_4 and TiO_2–Co_3O_4, a peak is observed in the pre-edge (7711 eV), which is absent in Co_3O_4. This peak becomes more intense when increasing the surface acidity of the oxide TiO_2 > ZnO. This peak is also characteristic of Co^{2+} in octahedral coordination (for which the lack of symmetry enhances the quadrupolar

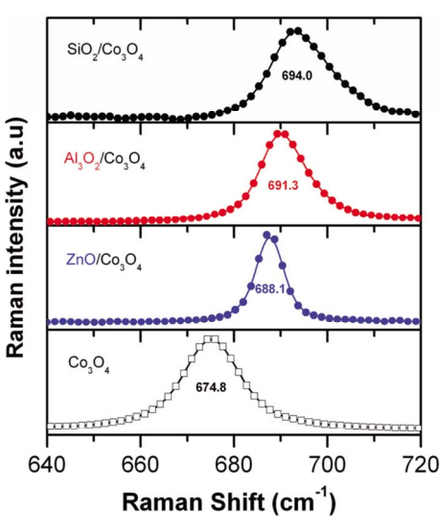

Figure 2. (Color online) Raman spectra comparison of pure Co_3O_4 treated at 400°C with mixtures of 1% of that Co_3O_4 with ZnO, Al_2O_3, and SiO_2 as milled without further thermal treatment.

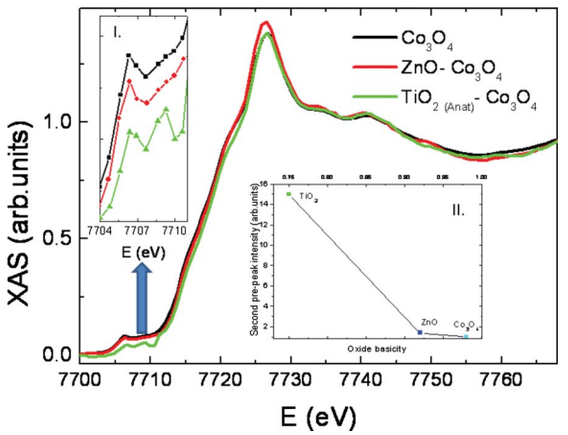

Figure 3. (Color online) X-ray absorption near-edge structure spectra at the Co K-edge for the samples of pure Co_3O_4 and mixtures of 5 wt % Co_3O_4 with ZnO and TiO_2, prepared under the same conditions. Insert I: magnification of the Co pre-edge area. Insert II: plot of the intensity of the second peak vs the theoretical oxide basicity.

transition).[20] These results are fully consistent and support the hypothesis that the magnetic signal arises from a partial reduction of Co^{3+} atoms in octahedral position to Co^{2+}.

A solid-state redox reaction then takes place at the surface of the Co_3O_4 when mixed with a dissimilar oxide such as ZnO and can be understood in terms of the high reactivity of the oxides surface. This is something well documented in heterogeneous catalysis and is dominated by the surface oxygen/hydroxyl ratio and the metal electronegativity. The presence of OH^- groups at the surface (among other species) is due to the hydroxylation of the M–O bonds (where M is the metallic cation) when exposed to the environment. Because the symmetry and coordination of the metal ions at the surface are lost, the ions show a strong tendency to be saturated by reacting with air molecules.[21] Therefore, all oxide surfaces at ambient conditions present an OH^-/O^{2-} ratio. This ratio is a "measurement" of the so-called basicity of the surface. Duffy[22] introduced the term for oxides, and since then, it has been extended to other systems such as silicates, borates, sulfides, fluorides, and phosphates. The optical basicity Λ expresses quantitatively the electron–donor power of O^{2-} atoms in oxides. Compounds where this electron density is low and with high content of OH^- in surface are acids. In other words, the higher the OH^-/O^{2-} ratio at the oxide surface, the more acidic the surface is. In heterogeneous catalysis, this acid–base behavior is used to explain the selective oxidation of different species such as hydrocarbons.[23]

According to the Λ scale[24] and with our spectroscopy measurements, ZnO is more acidic than Co_3O_4. Therefore, a priori, an acid–base neutralization reaction can occur while mixing the oxides. This process involves a chemical bond that is established between both surfaces Zn–OH $\cdots$ O–Co^{3+} during neutralization accompanied by a solid-state electron transference. An effective half-cell reaction for the Co_3O_4 can be described as

$$O^{2-} \rightarrow O^- + e^- \quad [1]$$

$$Co_{ss}^{3+} + e^- \rightarrow Co_{ss}^{2+} \quad [2]$$

where ss stands for the solid surface. These reactions give rise to the general solid-state electrochemical reaction of the type

$$Co_{ss}^{3+} + O^{2-} \rightarrow Co_{ss}^{2+} + O^- \quad [3]$$

A schematic illustration of the mechanism is shown in Fig. 4. This solid-state redox reaction accounts for the surface reduction of the Co_3O_4 nanoparticles when approaching the surface of ZnO particles during the low energy mixing. This process also allows the formation of oxygen vacancies at the interface if accompanied by a H_2O molecule loss.

The appearance of magnetic behavior in the Co_3O_4 nanoparticles after this surface reduction can be explained by taking into account that Co_3O_4 crystallizes in the spinel structure, like most of the ferrimagnetic materials as Fe_3O_4 and many other ferrites. In this structure, the primitive cell presents 8 Co^{2+} in tetrahedral (T) positions (surrounded by 4 oxygens) and 16 Co^{3+} in octahedral (O) positions (surrounded by 6 oxygens), as shown in Fig. 5a. However, Co_3O_4 is antiferromagnetic instead of ferrimagnetic with a Néel temperature of $\sim$30 K.[25,26] For spinel ferrites, the predominant magnetic interaction is the antiferromagnetic superexchange through oxygen atoms. The most intense interaction is T–O, which is antiferromagnetic, while the interactions T–T and O–O are also antiferromagnetic, but much weaker. Therefore, the atoms in T positions have a net ferromagnetic alignment (through the antiferromagnetic coupling with atoms in O positions) as Fig. 5b describes. As a consequence, there are two magnetic sublattices with antiparallel orientations: atoms in the T position and atoms in the O positions. As the magnetic moment of each sublattice is different, the result is the well-known ferrimagnetic behavior (see Fig. 5b).

The 3d level of the Co atoms in the presence of a crystal field with an octahedral symmetry splits in a doublet and in a triplet. The triplet has a lower energy, as Fig. 5c shows. The split is so large that Hund's rules do not apply and the population is described in Fig. 5c, giving rise to a zero magnetic moment. Therefore, for Co_3O_4, only atoms in the T position have nonzero magnetic moments. Consequently, there are no T–O interactions and the predominant interaction is T–T that is consistent with the antiferromagnetic behavior of the Co_3O_4. The splitting of the 3d level by the crystal field is due to the overlapping of the 3d orbital with the orbital of the surrounding atoms. Consequently, this splitting depends on the number and position of the surrounding atoms and the occupation of the 3d orbital. Figure 5d summarizes the result of the splitting for Co^{3+} and Co^{2+} in O positions. For the Co^{2+}, the splitting due to the crystal field in O positions is smaller than for Co^{3+} (about half of the value) and therefore Hund's rules apply so the magnetic moment is not zero.

The surface reduction of a Co^{3+} in the O position according to Reaction 2 modifies the crystal field (see Fig. 5e). This leads to a configuration of atoms Co^{2+} in O and Co^{2+} in T positions (as in Fe_3O_4). Then a nonzero magnetic moment appears in the T sublattice, and consequently the T–O interaction becomes the predominant one. In this situation, a ferrimagnetic behavior is estimated at the Co_3O_4 interface. The expected behavior is then paramagnetic with a ferrimagnetic component in agreement with the experimental data.

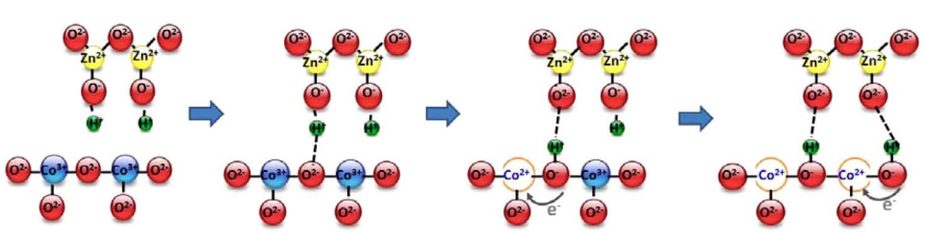

Figure 4. (Color online) Example of a schematic representation of a mechanism for a solid-state redox reaction taking place at the ZnO–Co_3O_4 oxide interfaces. The reduced cobalt (Co^{2+} in the octahedral position generated by the electrochemical reaction $Co_{ss}^{3+} + e^- \rightarrow Co_{ss}^{2+}$) is displayed in open circle (orange) with Co^{2+} inside where Co^{3+} in octahedral coordination is shown in a full dark circle (dark blue) with Co^{3+} inside.

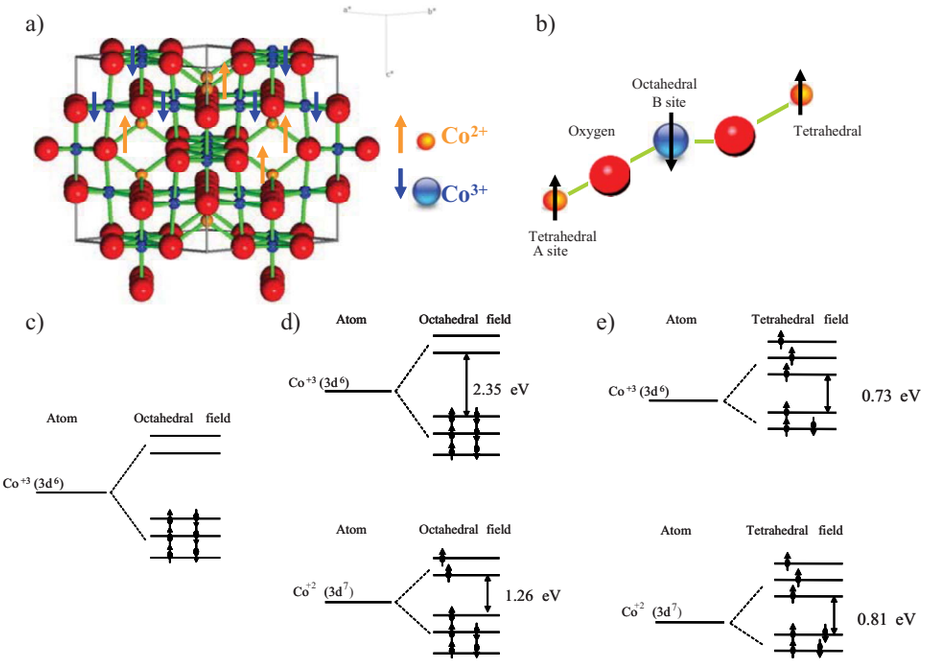

Figure 5. (Color online) (a) Co_3O_4 spinel structure [001] and arrows show the magnetic structure (A tetrahedral sites and B octahedral sites). (b) Ferromagnetic alignment of atoms in the tetrahedral position through the antiferromagnetic coupling with atoms in octahedral positions. (c) Splitting of the 3d level for Co^{3+} in the presence of an octahedral field leading to a zero spin value. (d) 3d level and population of Co^{3+} and Co^{2+} in the O symmetry. (e) 3d level and population of Co^{3+} and Co^{2+} in the T symmetry. Level configurations of cobalt in tetrahedral and octahedral cubic fields (Ref. 26) have been used.

This behavior is the one measured experimentally and reported here and explains the unusual properties found in mixtures of Co_3O_4 with ZnO.

The above-mentioned effect is intrinsic to a surface reduction of the Co_3O_4 nanoparticles and must be stabilized by the Co–O–Zn bonding formed at the interface because the magnetic response is still observed after heating the interfaces up at 700°C for several hours. The surface reduced Co_3O_4 nanoparticles also show a small magnetic contribution at room temperature that disappears at high temperatures.[18] Our explanation involves a difference in surface basicity between the two oxides. Taking into account that ZnO is an oxide with a low acidity compared with Co_3O_4, we assume that if more acidic oxides are chosen, then the magnetic properties of the interfaces should be magnified. To test this hypothesis the same amount of Co_3O_4 nanoparticles was mixed with more acidic oxides such as, α-Al_2O_3, anatase TiO_2, or quartz SiO_2. If the solid-state redox mechanism is responsible for the magnetic behavior, then these oxides should promote a stronger surface reduction and therefore a stronger room-temperature magnetic behavior and more stable Co–O–M bonds. Nevertheless, for further verification, pure Co_3O_4, ZnO, TiO_2, and Al_2O_3 powders were measured by IR spectroscopy to rate the acidic behavior in our powders, see Fig. 6.

According to Zecchina et al.,[27] bands in the region 3800–3650 cm^{-1} correspond to stretching modes of OH groups, which are not involved in hydrogen bonding. These groups include isolated OH and terminal hydroxyls of hydrogen-bonded sequences and are responsible for the electrochemical reduction. As observed, the one that presents a larger amount of OH groups is SiO_2, while Co_3O_4 has very few OH groups. This implies that a sequence of surface acidity can be established as follows

$$SiO_2 > Al_2O_3 > TiO_2 > ZnO > Co_3O_4$$

where SiO_2 is more acidic and the Co_3O_4 is more basic. Because this sequence is qualitative in the present study, we will use the theoretical optical basicity scale values.

To confirm that the electrochemical reduction observed depends on the acidic behavior of the oxide with which Co_3O_4 is mixed, oxide mixed with Co_3O_4, Al_2O_3, TiO_2, and SiO_2 powders with the same particle size that ZnO were low energy mixed with Co_3O_4 using the same particle size as ZnO. Room-temperature magnetic properties of the mixture without further thermal treatment were measured and are shown in Fig. 7.

All the mixtures exhibit a room-temperature paramagnetic component phase and a ferrimagnetic one. The hysteresis loops exhibit saturation magnetization values and coercivities larger than the previously observed for ZnO mixtures. Moreover, both coercivity and saturation magnetization values (H_c and M_s) scaled up with their optical acidity. These values also relate to the number of Co_3O_4 nanoparticles dispersed in the supporting oxide. Again, the dispersion of Co_3O_4 nanoparticles on the SiO_2 surface is of a higher number and better quality than the dispersion of Co_3O_4 on Al_2O_3 and at the same time better than in ZnO, as shown in Fig. 1d, c, and a, respectively. These experimental results confirm that a spontaneous redox electrochemical reaction occurs between oxides at the interfaces that establish Co–O–M chemical bonds and that the magnetism is a consequence of such reaction.

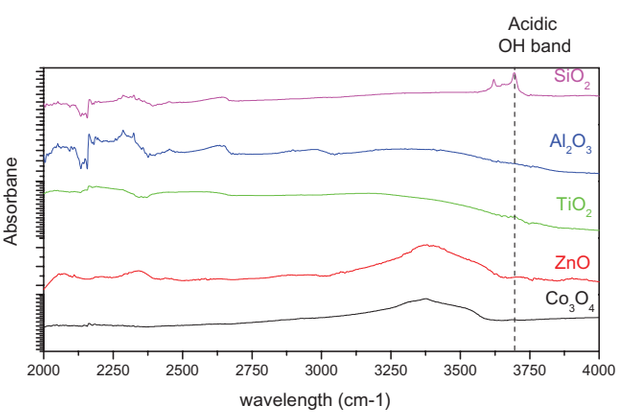

Figure 6. (Color online) IR spectra of Co_3O_4, ZnO, TiO_2, Al_2O_3, and SiO_2 powders before mixture or milling to check the basicity of their surfaces.

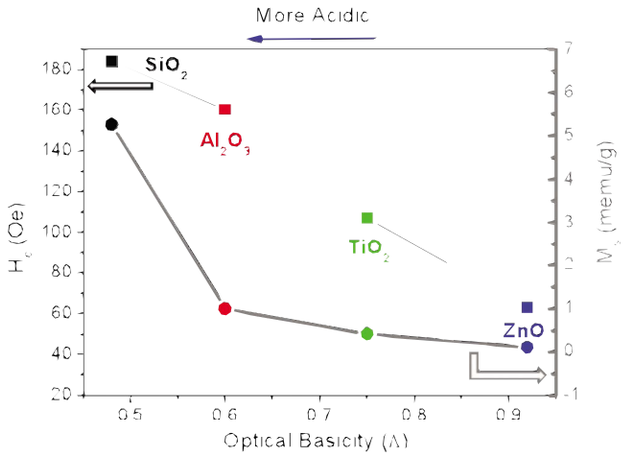

Figure 7. (Color online) Correlation between the theoretical optical basicity and the magnetic properties of interfaces prepared by milling for 5 min of ZnO, Al_2O_3, TiO_2, and SiO_2 with 1% Co_3O_4.

Conclusions

A spontaneous solid-state electrochemical reaction at the oxide nanoparticle interfaces such as ZnO/Co_3O_4, TiO_2/Co_3O_4, Al_2O_3/Co_3O_4, and SiO_2/Co_3O_4 mixtures can raise interesting properties such as the appearance of ferrimagnetic behavior. The mechanism by which the ordered magnetic phase appears is related to a surface reduction of the Co_3O_4 to CoO during mixing. This ferrimagnetic behavior is similar to that of ferrites with a spinel structure. This magnetism exists not only in semiconductors such as ZnO or TiO_2 (previously described in the literature) but also in other oxides with insulating properties such as SiO_2 or Al_2O_3. The strength of the interface reaction scales approximately with the difference in surface basicity of the oxides.

Interesting properties can be obtained at oxide surfaces by dry mixing for a few minutes that does not require complex preparation procedures or atomically flat surfaces. The presented reaction is also useful to deagglomerate particles without the need of liquids or dispersants that might modify the oxide particles. Finally, the idea of the surface reduction (or depletion of charge on the Co_3O_4 nanoparticles) could explain the origin of the magnetism observed in nanoparticles prepared by other methods.

Acknowledgments

This work was supported by the CSIC 2006-50F0122, CSIC 2007-50I015, FIS-2008-06249, MAT2008-06330, and CICYT MAT2007-66845-102-01. We acknowledge the European Synchrotron Radiation Facility for the provision of synchrotron radiation facilities and thank the SpLine CRG beamline staff for the assistance during X-ray absorption experiments. A. Quesada and F. Jimenez-Villacorta are acknowledged for the assistance with experimental work and fruitful discussions. J.L.C.-K. gratefully acknowledges the MMC at the University of Minnesota (Dan Dahlberg's group) and the MRSEC program for their support in magnetic measurements. M.S.M.G. also acknowledges the ERC program for her starting grant.

Instituto de Microelectrónica de Madrid assisted in meeting the publication costs of this article.

References

1. A. Brinkman, M. Huijben, M. van Zalk, J. Huijben, U. Zeitler, J. C. Maan, W. G. van der Wiel, G. Rijnders, D. H. A. Blank, and H. Hilgenkamp, *Nature Mater.*, **6**, 493 (2007).
2. F. Y. Bruno, J. Garcia-Barriocanal, M. Torija, A. Rivera, Z. Sefrioui, C. Leighton, C. Leon, and J. Santamaria, *Appl. Phys. Lett.*, **92**, 082106 (2008).
3. M. A. García, M. L. Ruiz-González, A. Quesada, J. L. Costa-Krämer, J. F. Fernández, S. J. Khatib, A. Wennberg, A. C. Caballero, M. S. Martín-González, M. Villegas, et al., *Phys. Rev. Lett.*, **94**, 217206 (2005).
4. A. Ohtomo and H. Y. Hwang, *Nature (London)*, **427**, 423 (2004).
5. N. Reyren, S. Thiel, A. D. Caviglia, L. Fitting Kourkoutis, G. Hammerl, C. Richter, C. W. Schneider, T. Kopp, A.-S. Rüetschi, D. Jaccard, et al., *Science*, **317**, 1196 (2007).
6. K. Urban, *Nature Mater.*, **5**, 173 (2006).
7. M. A. Ruderman and C. Kittel, *Phys. Rev.*, **96**, 99 (1954).
8. J. Kondo, *Prog. Theor. Phys.*, **32**, 37 (1964).
9. T. Dietl and H. Ohno, *Mater. Today*, **9**, 18 (2006).
10. K. Ando, *Science*, **312**, 1883 (2006); H. Ohno, *Science*, **281**, 951 (1998).
11. K. R. Kittilstved, N. S. Norberg, and D. R. Gamelin, *Phys. Rev. Lett.*, **94**, 147209 (2005).
12. J. M. D. Coey, M. Venkatesan, and C. B. Fitzgerald, *Nature Mater.*, **4**, 173 (2005).
13. K. R. Kittilstved and D. R. Gamelin, *J. Am. Chem. Soc.*, **127**, 5292 (2005).
14. K. R. Kittilstved, W. K. Liu, and D. R. Gamelin, *Nature Mater.*, **5**, 291 (2006).
15. M. S. Martín-González, J. F. Fernández, F. Rubio-Marcos, I. Lorite, J. L. Costa-Krämer, A. Quesada, M. A. Bañares, and J. L. G. Fierro, *J. Appl. Phys.*, **103**, 083905 (2008).
16. J. L. Costa-Krämer, F. Briones, J. F. Fernandez, A. C. Caballero, M. Villegas, M. Diaz, M. A. García, and A. Hernando, *Nanotechnology*, **16**, 214 (2005).
17. A. Quesada, M. A. García, M. Andrés, A. Hernando, J. F. Fernández, A. C. Caballero, M. S. Martín-González, and F. Briones, *J. Appl. Phys.*, **100**, 113909 (2006).
18. A. Serrano, E. Fernandez Pinel, A. Quesada, I. Lorite, M. Plaza, L. Pérez, F. Jiménez-Villacorta, J. de la Venta, M. S. Martín-González, J. L. Costa-Krämer, et al., *Phys. Rev. B*, **79**, 144405 (2009).
19. M. A. García, E. Fernández Pinel, J. de la Venta, A. Quesada, V. Bouzas, J. F. Fernández, J. J. Romero, M. S. Martín-González, and J. L. Costa-Krämer, *J. Appl. Phys.*, **105**, 013925 (2009).
20. A. Moen, D. G. Nicholson, M. Rnning, G. M. Lamble, J. F. Lee, and H. Emerich, *J. Chem. Soc., Faraday Trans.*, **93**, 4071 (1997).
21. *Metal Oxides: Chemistry and Applications*, J. L. Fierro, Editor, CRC Press, Boca Raton, FL (2005).
22. J. A. Duffy, *Geochim. Cosmochim. Acta*, **57**, 3961 (1993).
23. J. Vedrine, *Top. Catal.*, **21**, 97 (2002).
24. A. Lebouteiller and P. Courtine, *J. Solid State Chem.*, **137**, 94 (1998).
25. L. Hen, C. Chen, N. Wang, W. Zhou, and L. Guo, *J. Appl. Phys.*, **102**, 103911 (2007).
26. W. L. Roth, *J. Phys. Chem. Solids*, **25**, 1 (1964).
27. A. Zecchina, S. Bordiga, G. Spoto, L. Marchese, G. Petrini, G. Leofani, and M. Padovan, *J. Phys. Chem.*, **96**, 4985 (1992).